DOI: 10.1021/ic900757s

Inorganic Chemistry
Article

Heterometallic Complexes Based on the Mixed Bridging Ligands of Tricyanometalate and Terephthalate: Syntheses, Structures, and Magnetic Properties

Xiao-Ming Li, Cai-Feng Wang, Yong Ji, Ling-Chen Kang, Xin-Hui Zhou, Jing-Lin Zuo,* and Xiao-Zeng You

State Key Laboratory of Coordination Chemistry, School of Chemistry and Chemical Engineering, Nanjing National Laboratory of Microstructures, Nanjing University, Nanjing 210093, P.R. China.

Received April 20, 2009

With the use of the tailored tricyanometalate precursors $[(L)Fe(CN)_3]^-$ (L = Tp, tris(pyrazolyl)hydroborate; L = *i*-BuTp, 2-methylpropyltris(pyrazolyl)borate) and terephthalate (ta) units as the mixed bridging ligands, a new one-dimensional (1D) chain polymer $\{[(Tp)_2Fe_2(CN)_6Cu_2(ta)(dmbpy)_2]\cdot 7H_2O\}_n$ (**1**), a pentanuclear heterometallic cluster $[(Tp)_2Fe_2(CN)_6Cu_3(phen)_3(ta)_2(MeOH)(H_2O)_2]\cdot 8H_2O$ (**2**), and a tetranuclear heterometallic cluster $[(i\text{-}BuTp)_2Fe_2(CN)_6Cu_2(ta)(phen)_2(EtOH)_2]\cdot 2MeOH\cdot H_2O$ (**3**) (dmbpy = 4,4′-dimethyl-2,2′-bipyridyl, phen = 1,10-phenanthroline) have been synthesized and structurally characterized. The Fe^{III} and Cu^{II} ions are bridged by cyanides, and the Cu^{II} ions are further linked by terephthalate to form the 1D chain polymer, the pentanuclear cluster, and the tetranuclear cluster for complexes **1**−**3**, respectively. All complexes show ferromagnetic interactions between the Fe^{III} and Cu^{II} ions. Complex **1** shows metamagnetic behavior with the critical field of about 1.2 T at 1.8 K.

Introduction

Complexes with mixed bridging ligands have received much attention because of their fascinating structural architectures, such as one-dimensional (1D) chains, two-dimensional (2D) layers, and three-dimensional (3D) frameworks, and potential applications in the fields of catalysis, and magnetic and photo-materials.[1−3] A large number of complexes containing mixed bridging ligands hitherto have been reported, especially for the N- and O-mixed bridging ligands.[4] Among them, cyanide, a popular bridging ligand,[5] is able to mediate the magnetic interactions between two metal ions to some extent in the field of magnetic materials, such as single-molecular magnets,[6] single-chain magnets,[7]

*To whom correspondence should be addressed. E-mail: zuojl@nju.edu.cn. Fax: +86-25-83314502.

(1) (a) Bera, J. K.; Angaridis, P.; Cotton, F. A.; Petrukhina, M. A.; Fanwick, P. E.; Walton, R. A. *J. Am. Chem. Soc.* **2001**, *123*, 1515. (b) Batten, S. R.; Murray, K. S. *Coord. Chem. Rev.* **2003**, *246*, 103. (b) Ye, B. H.; Tong, M. L.; Chen, X. M. *Coord. Chem. Rev.* **2005**, *249*, 545.

(2) (a) Lu, J. Y.; Lawandy, M. A.; Li, J.; Yuen, T.; Lin, C. L. *Inorg. Chem.* **1999**, *38*, 2695. (b) Das, N.; Mukherjee, P. S.; Arif, A. M.; Stang, P. J. *J. Am. Chem. Soc.* **2003**, *125*, 13950. (c) Zhang, X. M.; Tong, M. L.; Chen, X. M. *Angew. Chem., Int. Ed.* **2002**, *41*, 1029.

(3) (a) Lin, W. B.; Wang, Z. Y.; Ma, L. *J. Am. Chem. Soc.* **1999**, *121*, 11249. (b) Liao, Y. C.; Liao, F. L.; Chang, W. K.; Wang, S. L. *J. Am. Chem. Soc.* **2004**, *126*, 1320. (c) Choi, H. J.; Suh, M. P. *J. Am. Chem. Soc.* **2004**, *126*, 15844.

(4) (a) Tao, J.; Yin, X.; Huang, R. B.; Zheng, L. S. *Inorg. Chem. Commun.* **2002**, *5*, 1000. (b) Kitagawa, S.; Okubo, T.; Kawata, S.; Kondo, M.; Katada, M.; Kobayashi, H. *Inorg. Chem.* **1995**, *34*, 4790. (c) Shi, Z.; Zhang, L. R.; Gao, S.; Yang, G. Y.; Hua, J.; Gao, L.; Feng, S. H. *Inorg. Chem.* **2000**, *39*, 1990. (d) Geraghty, M.; Sheridan, V.; McCanna, M.; Devereuxb, M.; McKee, V. *Polyhedron.* **1999**, *18*, 2931. (e) Hao, N.; Shen, E. H.; Li, Y. G.; Wang, E. B.; Hu, C. W.; Xu, L. *Inorg. Chem. Commun.* **2004**, *7*, 510.

(5) (a) Dunbar, K. R.; Heintz, R. A. *Prog. Inorg. Chem.* **1997**, *45*, 283. (b) Weihe, H.; Güdel, H. U. *Comments Inorg. Chem.* **2000**, *22*, 75. (c) Miller, J. S. *MRS. Bull.* **2000**, *25*, 60. (d) Marvaud, V.; Decroix, C.; Scuiller, A.; Guyard-Duhayon, C.; Vaissermann, J.; Gonnet, F.; Verdaguer, M. *Chem.—Eur. J.* **2003**, *9*, 1677. (e) Marvaud, V.; Decroix, C.; Scuiller, A.; Tuyèras, F.; Guyard-Duhayon, C.; Vaissermann, J.; Marrot, J.; Gonnet, F.; Verdaguer, M. *Chem.—Eur. J.* **2003**, *9*, 1692. (f) Beltran, L. M. C.; Long, J. R. *Acc. Chem. Res.* **2005**, *38*, 325 and references therein.

(6) (a) Schelter, E. J.; Prosvirin, A. V.; Reiff, W. M.; Dunbar, K. R. *Angew. Chem., Int. Ed.* **2004**, *43*, 4912. (b) Berlinguette, C. P.; Vaughn, D.; Cañada-Vilalta, C.; Galán-Mascarós, J. R.; Dunbar, K. R. *Angew. Chem., Int. Ed.* **2003**, *42*, 1523. (c) Sokol, J. J.; Hee, A. G.; Long, J. R. *J. Am. Chem. Soc.* **2002**, *124*, 7656. (d) Larionova, J.; Gross, M.; Pilkington, M.; Andres, H.; Stoeckli-Evans, H.; Güdel, H. U.; Decurtins, S. *Angew. Chem., Int. Ed.* **2000**, *39*, 1605. (e) Wang, S.; Zuo, J. L.; Zhou, H. C.; Choi, H. J.; Ke, Y.; Long, J. R.; You, X. Z. *Angew. Chem., Int. Ed.* **2004**, *43*, 5940. (f) Wang, C. F.; Zuo, J. L.; Bartlett, B. M.; Song, Y.; Long, J. R.; You, X. Z. *J. Am. Chem. Soc.* **2006**, *128*, 7162. (g) Li, D. F.; Parkin, S.; Wang, G. B.; Yee, G. T.; Clérac, R.; Wernsdorfer, W.; Holmes, S. M. *J. Am. Chem. Soc.* **2006**, *128*, 4214.

(7) (a) Wang, S.; Zuo, J. L.; Gao, S.; Song, Y.; Zhou, H. C.; Zhang, Y. Z.; You, X. Z. *J. Am. Chem. Soc.* **2004**, *126*, 8900. (b) Lescouëzec, R.; Vaissermann, J.; Ruiz-Pérez, C.; Lloret, F.; Carrasco, R.; Julve, M.; Verdaguer, M.; Dromzee, Y.; Gatteschi, D.; Wernsdorfer, W. *Angew. Chem., Int. Ed.* **2003**, *42*, 1483. (c) Lescouëzec, R.; Lloret, F.; Julve, M.; Vaissermann, J.; Verdaguer, M. *Inorg. Chem.* **2002**, *41*, 818. (d) Coulon, C.; Miyasaka, H.; Clérac, R. *Struct. Bonding* (*Berlin*) **2006**, *122*, 163 and references therein. (e) Ferbinteanu, M.; Miyasaka, H.; Wernsdorfer, W.; Nakata, K.; Sugiura, K.; Yamashita, M.; Coulon, C.; Clérac, R. *J. Am. Chem. Soc.* **2005**, *127*, 3090.

Published on Web 08/27/2009

photoinduced magnetic materials,[8] or spin-crossover magnets.[9] The tailored tricyanometalate precursor $[(Tp)Fe(CN)_3]^-$ (Tp = tris(pyrazolyl)hydroborate) becomes one of the versatile building blocks for the following reasons: (i) $[(Tp)Fe(CN)_3]^-$, bearing a negative charge, exhibits the virtue of good solubility and provides high-spin products with lower positive charge and improved stability; (ii) the low-spin Fe(III) ion in $[(Tp)Fe(CN)_3]^-$ has obvious influence on the magnetic anisotropy of resulting complexes because of its unquenched first-order orbital angular momentum.[10] With the use of tris(pyrazolyl)borate iron(III) tricyanide as the precursor, some lower-dimensional heterometallic complexes with interesting magnetic properties have been obtained.[11−16] On the other hand, carboxylate ligands, which are able to link two or more metal ions either in monodentate or in bidentate modes, are also playing an important role in coordination chemistry, justified by not only the fascinating topological structures and stabilities of the complexes but also their tremendously useful applications.[17,18]

Scheme 1

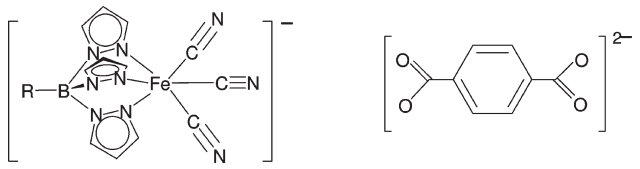

Tp (R= H)
***i*-BuTp (R = *i*-Bu)** **ta**

To extend the research on metal complexes with mixed bridging ligands, we are trying to synthesize complexes with the use of hybrid bridging ligands of carboxylate and tricyanometalate building blocks (Scheme 1). In this paper, the reactions of $Cu(ClO_4)_2 \cdot 6H_2O$, ta (ta = terephthalate), the auxiliary ligands (dmbpy or phen, dmbpy = 4,4′-dimethyl-2,2′-bipyridyl, phen = 1,10-phenanthroline) and $[(Tp)Fe(CN)_3]^-$ or $[(i\text{-BuTp})Fe(CN)_3]^-$, afford three interesting complexes: the 1D chain polymer $\{[(Tp)_2Fe_2(CN)_6Cu_2(ta)(dmbpy)_2] \cdot 7H_2O\}_n$ (**1**), the pentanuclear heterometallic cluster $[(Tp)_2Fe_2(CN)_6Cu_3(phen)_3(ta)_2(MeOH)(H_2O)_2] \cdot 8H_2O$ (**2**), and the tetranuclear heterometallic cluster $[(i\text{-BuTp})_2Fe_2(CN)_6Cu_2(ta)(phen)_2(EtOH)_2] \cdot 2MeOH \cdot H_2O$ (**3**). The structures of these products differ dramatically by using different auxiliary ligands and tricyanometalate building blocks. Herein, their structures and magnetic properties are also described.

Experimental Section

Materials and Physical Measurements. All chemicals and solvents were commercially available, analytical reagent-grade, and used as received. $(Bu_4N)[(Tp)Fe(CN)_3]$,[11a] $(Bu_4N)[(i\text{-BuTp})Fe(CN)_3]$,[12b] and peperidinium terephthalate[19] were synthesized according to the literature methods. Elemental analyses for C, H, and N were performed on a CHN-O-Rapid analyzer and an Elementar Vario MICRO analyzer. Infrared spectra were recorded on a Vector22 Bruker spectrophotometer with KBr pellets in the 400−4000 cm^{-1} region.

Caution! The cyanides are very toxic, and perchlorate salts are potentially explosive. Thus, these starting materials should be handled in small quantities and with great caution.

Preparation of $\{[(Tp)_2Fe_2(CN)_6Cu_2(ta)(dmbpy)_2] \cdot 7H_2O\}_n$ (1). A methanol solution (2 mL) of $(Bu_4N)[(Tp)Fe(CN)_3]$ (12 mg, 0.02 mmol) was added to a solution (2 mL of methanol and 1 mL of water) containing $Cu(ClO_4)_2 \cdot 6H_2O$ (7.5 mg, 0.02 mmol) and dmbpy (3.2 mg, 0.02 mmol). A mixture of methanol and water (v:v = 5:1, 6 mL) was carefully layered on the top of the above solution. The methanol solution (0.02 mol·L^{-1}, 1 mL) of terephthalate/triethylamine (mole ratio = 1:2) was gently added as the third layer. Brown block-shaped crystals of complex **1** were obtained in 1 week. Yield: 7.0 mg (47%). Anal. Calcd for $C_{56}H_{62}B_2Cu_2Fe_2N_{22}O_{11}$ (%): C, 45.45; H, 4.22; N, 20.82. Found: C, 45.61; H, 4.25; N, 20.69. IR (KBr, cm^{-1}): 3115(br, m), 2158 (m), 2122(m), 1618 (s), 1594 (s), 1407 (s), 1359 (s), 1313 (s), 1288 (s), 1213(s), 1048(s), 830 (m), 774 (m), 710 (m).

$[(Tp)_2Fe_2(CN)_6Cu_3(phen)_3(ta)_2(MeOH)(H_2O)_2] \cdot 8H_2O$ (2). Solid $Cu(ClO_4)_2 \cdot 6H_2O$ (7.5 mg, 0.02 mmol) and phen (4.3 mg, 0.02 mmol) were dissolved in 2 mL of methanol and water (v:v = 1:1). A solution of methanol and water (v:v = 5:1, 6 mL) was

(8) (a) Arimoto, Y.; Ohkoshi, S. I.; Zhong, Z. J.; Seino, H.; Mizobe, Y.; Hashimoto, K. *J. Am. Chem. Soc.* **2003**, *125*, 9240. (b) Rombaut, G.; Verelst, M.; Golhen, S.; Ouahab, L.; Mathoniere, C.; Kahn, O. *Inorg. Chem.* **2001**, *40*, 1151. (c) Herrera, J. M.; Marvaud, V.; Verdaguer, M.; Marrot, J.; Kalisz, M.; Mathonière, C. *Angew. Chem., Int. Ed.* **2004**, *43*, 5468. (d) Li, D. F.; Clérac, R.; Roubeau, O.; Harté, E.; Mathonière, C.; Bris, R. L.; Holmes, S. M. *J. Am. Chem. Soc.* **2008**, *130*, 252.

(9) (a) Niel, V.; Thompson, A. L.; Muñoz, M. C.; Galet, A.; Goeta, A. E.; Real, J. A. *Angew. Chem., Int. Ed.* **2003**, *42*, 3760. (b) Niel, V.; Galet, A.; Gaspar, A. B.; Muñoz, M. C.; Real, J. A. *Chem. Commun.* **2003**, 1248. (c) Niel, V.; Martinez-Agudo, J. M.; Muñoz, M. C.; Gaspar, A. B.; Real, J. A. *Inorg. Chem.* **2001**, *40*, 3838. (d) Shatruk, M.; Dragulescu-Andrasi, A.; Chambers, K. E.; Stoian, S. A.; Bominaar, E. L.; Achim, C.; Dunbar, K. R. *J. Am. Chem. Soc.* **2007**, *129*, 6104.

(10) (a) Palii, A. V.; Ostrovsky, S. M.; Klokishner, S. I.; Tsukerblat, B. S.; Dunbar, K. R. *Chem. Phys. Chem.* **2006**, *7*, 871. (b) Park, K.; Holmes, S. M. *Phys. Rev. B.* **2006**, *74*, 224440.

(11) (a) Lescouëzec, R.; Vaissermann, J.; Lloret, F.; Julve, M.; Verdaguer, M. *Inorg. Chem.* **2002**, *41*, 5943. (b) Lescouëzec, R.; Toma, L. M.; Vaissermann, J.; Verdaguer, M.; Delgado, F. S.; Ruiz-Pérez, C.; Lloret, F.; Julve, M. *Coord. Chem. Rev.* **2005**, *249*, 2691.

(12) (a) Wen, H. R.; Wang, C. F.; Song, Y.; Gao, S.; Zuo, J. L.; You, X. Z. *Inorg. Chem.* **2006**, *45*, 8942. (b) Wang, C. F.; Liu, W; You Song, Y.; Zhou, X. H.; Zuo, J. L.; You, X. Z. *Eur. J. Inorg. Chem.* **2008**, 717. (c) Liu, W.; Wang, C. F.; Li, Y. Z.; Zuo, J. L.; You, X. Z. *Inorg. Chem.* **2006**, *45*, 10058. (d) Gu, Z. G.; Yang, Q. F.; Liu, W.; Song, Y.; Li, Y. Z.; Zuo, J. L.; You, X. Z. *Inorg. Chem.* **2006**, *45*, 8895. (e) Wang, S.; Zuo, J. L.; Zhou, H. C.; Song, Y.; Gao, S.; You, X. Z. *Eur. J. Inorg. Chem.* **2004**, 3681.

(13) (a) Jiang, L.; Feng, X. L.; Lu, T. B.; Gao, S. *Inorg. Chem.* **2006**, *45*, 5018. (b) Jiang, L.; Choi, H. J.; Feng, X. L.; Lu, T. B.; Long, J. R. *Inorg. Chem.* **2007**, *46*, 2181.

(14) (a) Kim, J.; Han, S.; Cho, I. K.; Choi, K. Y.; Heu, M.; Yoon, S.; Suh, B. J. *Polyhedron* **2004**, *23*, 1333. (b) Kim, J.; Han, S.; Pokhodnya, K. I.; Migliori, J. M.; Miller, J. S. *Inorg. Chem.* **2005**, *44*, 6983.

(15) (a) Li, D. F.; Parkin, S.; Wang, G.; Yee, G. T.; Holmes, S. M. *Inorg. Chem.* **2006**, *45*, 1951. (b) Li, D. F.; Parkin, S.; Wang, G.; Yee, G. T.; Holmes, S. M. *Inorg. Chem.* **2006**, *45*, 2773. (c) Li, D. F.; Parkin, S.; Clérac, R.; Holmes, S. M. *Inorg. Chem.* **2006**, *45*, 7569. (d) Li, D. F.; Parkin, S.; Wang, G.; Yee, G. T.; Prosvirin, A. V.; Holmes, S. M. *Inorg. Chem.* **2005**, *44*, 4903. (e) Li, D. F.; Clérac, R.; Parkin, S.; Wang, G. B.; Yee, G. T.; Holmes, S. M. *Inorg. Chem.* **2006**, *45*, 5251. (f) Li, D. F.; Clérac, R.; Wang, G. B.; Yee, G. T.; Holmes, S. M. *Eur. J. Inorg. Chem.* **2007**, 1341.

(16) (a) Harris, T. D.; Long, J. R. *Chem. Commun.* **2007**, 1360. (b) Kwak, H. Y.; Ryu, D. W.; Kim, H. C.; Koh, E. K.; Cho, B. K.; Hong, C. S. *Dalton Trans.* **2009**, 1954. (c) Wang, S.; Ferbinteanu, M.; Yamashita, M. *Inorg. Chem.* **2007**, *46*, 610. (d) Kim, J. I.; Kwak, H. Y.; Yoon, J. H.; Ryu, D. W.; Yoo, I. Y.; Yang, N.; Cho, B. K.; Park, J. G.; Lee, H.; Hong, C. S. *Inorg. Chem.* **2009**, *48*, 2956.

(17) (a) Wang, X. Y.; Gan, L.; Zhang, S. W.; Gao, S. *Inorg. Chem.* **2004**, *43*, 4615. (b) Cao, R.; Sun, D. F.; Liang, Y. C.; Hong, M. C.; Tatsumi, K.; Shi, Q. *Inorg. Chem.* **2002**, *41*, 2087. (c) Liu, Y. H.; Lu, Y. L.; Wu, H. C.; Wang, J. C.; Lu, K. L. *Inorg. Chem.* **2002**, *41*, 2592.

(18) (a) Bakalbassis, E. G.; Mrozinski, J.; Tsipis, C. A. *Inorg. Chem.* **1986**, *25*, 684. (b) Cheng, P.; Yan, S. P.; Xie, C. Z.; Zhao, B.; Chen, X. Y.; Liu, X. W.; Li, C. H.; Liao, D. Z.; Jiang, Z. H.; Wang, G. L. *Eur. J. Inorg. Chem.* **2004**, 2369. (c) Hong, C. S.; Yoon, J. H.; Lim, J. H.; Ko, H. H. *Eur. J. Inorg. Chem.* **2005**, 4818. (d) Shen, W. Z.; Chen, X. Y.; Cheng, P.; Yan, S. P.; Zhai, B.; Liao, D. Z.; Jiang, Z. H. *Eur. J. Inorg. Chem.* **2005**, 2297.

(19) Verdaguer, M.; Gouteron, J.; Jeannin, S.; Jeannin, Y.; Kahn, O. *Inorg. Chem.* **1984**, *23*, 4291.

Table 1. Summary of Crystallographic Data for the Complexes **1**−**3**

	1	**2**	**3**
formula	$C_{56}H_{62}B_2Cu_2Fe_2N_{22}O_{11}$	$C_{77}H_{76}B_2Cu_3Fe_2N_{24}O_{19}$	$C_{70}H_{78}B_2Cu_2Fe_2N_{22}O_9$
M_r	1479.68	1965.56	1631.94
cryst syst	triclinic	orthorhombic	triclinic
space group	$P\bar{1}$	*Pnma*	$P\bar{1}$
a, Å	11.9584(16)	34.693(5)	9.569(2)
b, Å	12.3382(17)	39.556(5)	12.246(3)
c, Å	13.2513(18)	7.6751(11)	16.744(4)
α, deg	84.083(3)	90.00	98.490(4)
β, deg	65.274(2)	90.00	92.007(4)
γ, deg	69.814(2)	90.00	110.561(4)
V, Å^3	1664.9(4)	10533(3)	1809.0(7)
Z	1	4	1
ρ_c, g cm^{-3}	1.476	1.240	1.498
F(000)	760	4028	844
T, K	291(2)	291(2)	293(2)
μ, mm^{-1}	1.131	0.932	1.046
index ranges	$-14 \le h \le 14$ $-11 \le k \le 15$ $-16 \le l \le 16$	$-41 \le h \le 42$ $-39 \le k \le 48$ $-9 \le l \le 9$	$-12 \le h \le 11$ $-15 \le k \le 13$ $-21 \le l \le 16$
data/restraints/ parameters	6373/0/ 442	3245/0/628	7590/0/ 488
GOF (F^2)	1.012	1.044	1.089
$R_1{}^a$, $\omega R_2{}^b$ ($I > 2\sigma(I)$)	0.0584, 0.1390	0.0638, 0.1190	0.0622, 0.1732
$R_1{}^a$, $\omega R_2{}^b$(all data)	0.0784, 0.1486	0.1033, 0.1297	0.0717, 0.1806

$^a R_1 = \sum||F_o| - |F_c||/\sum|F_o|$. $^b R_2 = [\sum w(F_o^2 - F_c^2)^2/\sum w(F_o^2)]^{1/2}$

carefully layered on the top of the above solution. Another mixture of peperidinium terephthalate (7 mg, 0.02 mmol) and $(Bu_4N)[(Tp)Fe(CN)_3]$ (12 mg, 0.02 mmol) in 3 mL of methanol was added carefully as the third layer. Brown block-shaped crystals of complex **2** were obtained in 4 days. Yield: 6.8 mg (52% based on Cu). Anal. Calcd for $C_{77}H_{76}B_2Cu_3Fe_2N_{24}O_{19}$ (%): C, 47.05; H, 3.90; N, 17.10. Found: C, 47.11; H, 3.93; N, 17.04. IR (KBr, cm^{-1}): 3123 (br, m), 2169 (m), 2123 (m), 1588 (s), 1500 (m), 1427 (s), 1407(s), 1361 (s), 1341(s), 1313 (s), 1213 (s), 1074 (s), 851 (m), 796 (s), 764 (s).

$[(i\text{-BuTp})_2Fe_2(CN)_6Cu_2(ta)(phen)_2(EtOH)_2]\cdot 2MeOH\cdot H_2O$ (3). A mixture of methanol and water (v/v = 5:1, 6 mL) was gently layered on the top of a solution of $Cu(ClO_4)_2\cdot 6H_2O$ (7.5 mg, 0.02 mmol) and phen (4.3 mg, 0.02 mmol) in 2 mL of methanol and 1 mL of water. Another mixture of $(Bu_4N)[(i\text{-BuTp})Fe(CN)_3]$ (13 mg, 0.02 mmol) in 2 mL of ethanol/methanol (v/v = 1:1) and methanol solution (0.02 mol·L^{-1}, 1 mL) of terephthalate/triethylamine (mole ratio = 1:2) were added carefully as the third layer. Brown block crystals of complex **3** were obtained after 3 days. Yield: 8.3 mg (51%). Anal. Calcd for $C_{70}H_{78}B_2Cu_2Fe_2N_{22}O_9$ (%): C, 51.51; H, 4.81; N, 18.88. Found: C, 51.65; H, 4.83; N, 18.76. IR (KBr, cm^{-1}): 3150 (br, m), 2958 (br, m), 2871 (br, m), 2175 (m), 2128 (m), 1598 (s), 1519 (s), 1501 (s), 1428 (s), 1409 (s), 1386 (s), 1341 (s), 1302 (s), 1110 (s), 1064 (s), 850 (m), 761 (s), 723 (s).

X-ray Crystallography. The crystal structures of complexes **1**−**3** were determined on a Siemens (Bruker) SMART CCD diffractometer using monochromated Mo Kα radiation (λ = 0.71073 Å) at room temperature. Cell parameters were retrieved using the SMART software and refined using SAINT[20] on all observed reflections. Data was collected using a narrow-frame method with scan widths of 0.30° in ω and an exposure time of 10 s/frame. The highly redundant data were reduced using SAINT and corrected for Lorentz and polarization effects. Absorption corrections were applied using SADABS[21] supplied by Bruker. Structures were solved by direct methods using the program SHELXL-97.[22] The positions of the metal atoms and their first coordination spheres were located from direct-method E maps; other non-hydrogen atoms were found using alternating difference Fourier syntheses and least-squares refinement cycles and, during the final cycles, were refined anisotropically. Hydrogen atoms were placed in calculated positions and refined as riding atoms with a uniform value of U_{iso}. Information concerning crystallographic data collection and structure refinement is summarized in Table 1. Selected bond lengths and angles for **1**−**3** are given in Table 2.

Magnetic Susceptibility Measurements. The magnetic susceptibility measurements for all crystalline samples were measured over the temperature range of 1.8−300 K with a Quantum Design MPMS-XL7 SQUID magnetometer using an applied magnetic field of 2000 Oe. Field dependences of magnetization were measured up to 70 kOe (7 T). Data were corrected for the diamagnetic contribution calculated from Pascal constants. The alternating current (AC) measurements were performed at various frequencies from 1 to 1500 Hz with the AC field amplitude of 5 Oe and no direct current (DC) field applied.

Results and Discussion

Syntheses. In this paper, the anionic precursors, $[(Tp)Fe(CN)_3]^-$ and the analogous $[(i\text{-BuTp})Fe(CN)_3]^-$, are chosen as the cyano-bridged building blocks; and μ-(terephthalato) is chosen as O bridging ligand. They are chosen to prepare polynuclear clusters and coordination polymers with mixed bridging ligands. The self-assembly reaction of $Cu(ClO_4)_2\cdot 6H_2O$, the auxiliary ligand dmbpy, $(Bu_4N)[(Tp)Fe(CN)_3]$ and terephthalate/triethylamine (mole ratio = 1:2) in methanol/water mixture yields the novel 1D polymeric heterometallic complex, $\{[(Tp)_2Fe_2(CN)_6Cu_2(ta)(dmbpy)_2]\cdot 7H_2O\}_n$ (**1**). The pentanuclear complex $[(Tp)_2Fe_2(CN)_6Cu_3(phen)_3(ta)_2(MeOH)(H_2O)_2]\cdot 8H_2O$ (**2**) is synthesized from $Cu(ClO_4)_2\cdot 6H_2O$, auxiliary ligand phen, $(Bu_4N)[(Tp)Fe(CN)_3]$, and peperidinium terephthalate. However, with the similar reaction conditions as the preparation of compound **1**, by using $(Bu_4N)[(i\text{-BuTp})Fe(CN)_3]$ and phen instead of $(Bu_4N)[(Tp)Fe(CN)_3]$ and dmbpy, the final product is the tetranuclear complex $[(i\text{-BuTp})_2Fe_2(CN)_6Cu_2(ta)(phen)_2(EtOH)_2]\cdot 2MeOH\cdot H_2O$ (**3**). To the best of our knowledge, there is still no example of polynuclear complexes with both carboxylates and tricyanometalate bridging ligands reported before.

In the IR absorption spectra, the stretching vibrations of C≡N are observed at 2158 and 2122 cm^{-1} for **1**, 2169 and 2123 cm^{-1} for **2**, and 2175 and 2128 cm^{-1} for **3**, respectively, which are in agreement with the presence of the bridging and terminal cyanide ligands. The strong absorption peaks located at 1618 and 1359 cm^{-1} for **1**, 1588 and 1361 cm^{-1} for **2**, and 1598 and 1386 cm^{-1} for **3**, are related to antisymmetric $\nu_{as}(COO^-)$ and symmetric $\nu_s(COO^-)$ stretching vibrations, respectively. The differences ($\Delta\nu$) between $\nu_{as}(COO^-)$ and $\nu_s(COO^-)$ (259 cm^{-1} for **1**, 227 cm^{-1} for **2** and 212 cm^{-1} for **3**, respectively) are indicative of the amphimonodentate coordination mode of terephthalate dianion in all of three complexes,[18c,23]

(20) *SAINT-Plus*, version 6.02; Bruker Analytical X-ray System: Madison, WI, 1999.

(21) Sheldrick, G. M. *SADABSs An empirical absorption correction program*; Bruker Analytical X-ray Systems: Madison, WI, 1996.

(22) Sheldrick, G. M. *SHELXTL-97*; Universität of Göttingen: Göttingen, Germany, 1997.

(23) (a) Xanthopoulos, C. E.; Sigalas, M. P.; Katsoulos, G. A.; Tsipis, C. A.; Terzis, A.; Mentzafos, M.; Hountas, A. *Inorg. Chem.* **1993**, *32*, 5433. (b) Shakhatreh, S. K.; Bakalbassis, E. G.; Bruedgam, I.; Hartl, H.; Mrozinski, J.; Tsipis, C. A. *Inorg. Chem.* **1991**, *30*, 2801. (c) Bakalbassis, E. G.; Mrozinski, J.; Tsipis, C. A. *Inorg. Chem.* **1986**, *25*, 3684.

Table 2. Selected Bond Lengths (Å) and Angles (deg) for Complexes **1**−**3**

			1		
Cu1−O1	1.930(3)	Cu1−N9	1.997(4)	Cu1−N10	2.003(4)
Cu1−N11	2.024(4)	Cu1−N7[a]	2.247(4)	Fe1−C10	1.912(5)
Fe1−C12	1.920(5)	Fe1−C11	1.932(5)	Fe1−N2	1.957(4)
Fe1−N6	1.968(4)	Fe1−N4	1.985(4)	C12−N9	1.146(5)
C10−N7	1.150(5)	C11−N8	1.142(6)	O1−Cu1−N10	171.65(14)
C10−N7−Cu1[a]	150.6(4)	C12−N9−Cu1	159.5(3)	C25−O1−Cu1	120.2(3)
N8−C11− Fe1	177.2(5)	N7−C10−Fe1	175.8(4)	N9−C12−Fe1	174.5(4)
C12−Fe1−N2	93.41(16)	C12−Fe1−N6	175.98(16)	O2−C25−O1	124.5(5)
C10−Fe1−C12	86.90(18)	C10−Fe1−C11	90.80(19)	O1−Cu1−N9	93.71(14)
O1−Cu1− N7[a]	87.77(14)	N10−Cu1−N7[a]	96.29(15)	N11−Cu1−N7[a]	100.89(14)
N9−Cu1− N7[a]	94.62(15)	N9−Cu1−N10	93.23(15)	C12−Fe1−C11	87.27(18)
			2		
C10−Fe1	2.047(4)	C11−Fe1	1.995(4)	C12−Fe1	1.891(5)
C10−N7	1.000(4)	Fe1−N1	1.887(3)	Fe1−N5	2.000(3)
Fe1−N3	2.010(3)	Cu1−N7	1.976(4)	Cu1−O1	1.990(3)
Cu1−O6	2.302(3)	Cu1−N10	2.036(3)	Cu1−N11	2.069(3)
Cu2−O3	1.986(3)	Cu2−N12	1.994(3)	Cu2−O5	2.253(4)
N7−C10−Fe1	169.8(4)	N8−C11−Fe1	166.8(4)	N9−C12−Fe1	168.5(4)
C10−N7−Cu1	176.6(4)	C32−O3−Cu2	126.6(3)	O1−Cu1−O6	102.94(11)
N10−Cu1−O6	87.82(11)	N11−Cu1−O6	92.93(12)	O3−Cu2−O5	101.59(11)
N12−Cu2−O5	78.98(12)	N7−Cu1−O6	93.75(12)		
			3		
Cu1−O2	1.901(3)	Cu1−O3	2.218(3)	Cu1−N1	1.944(3)
Cu1−N10	2.021(3)	Cu1−N11	2.006(3)	Fe1−C1	1.906(4)
Fe1−C2	1.917(4)	Fe1−C3	1.923(4)	Fe1−N8	1.951(3)
Fe1−N4	1.964(3)	Fe1−N6	1.965(3)	C1−N1	1.147(5)
C2−N2	1.125(6)	C3−N3	1.135(5)	O2−Cu1−O3	90.04(12)
O2−Cu1−N1	94.48(13)	O2−Cu1−N10	171.61(13)	O2−Cu1−N11	90.83(13)
N11−Cu1−N10	80.95(13)	N11−Cu1−O3	95.09(12)	N1−Cu1−O3	97.79(13)
N1−Cu1−N11	166.05(13)	N10−Cu1−O3	92.36(12)	C1−N1−Cu1	172.6(3)
N1−C1−Fe1	175.3(3)	C1−Fe1−C2	84.81(17)	C1−Fe1−C3	87.14(17)
C1−Fe1−N8	93.44(14)	C1−Fe1−N4	176.96(14)	C1−Fe1−N6	94.32(14)
C2−Fe1−C3	88.67(18)	C2−Fe1−N4	92.46(16)	C29−O2−Cu1	123.1(3)
O1−C29−O2	124.9(4)	N2−C2−Fe1	176.0(4)	N3−C3−Fe1	178.2(4)

[a] Symmetry operation: $2 - x, -y, 1 - z$.

which was confirmed by structural analyses as described later.

Structural Description. The crystal structure for complex **1** is depicted in Figure 1. It shows the 1D heterometallic chain structure consisting of the basic rectangular units $[(Tp)_2Fe_2(CN)_6Cu_2(dmbpy)_2]^{2+}$ linked by terephthalate dianions, where Fe^{III} and Cu^{II} ions are located at alternating situations of the rectangle. In the rectangle unit, each Cu^{II} ion is linked to two $[(Tp)Fe(CN)_3]^-$ units at *cis* positions, while each $[(Tp)Fe(CN)_3]^-$ unit uses two of its three cyanide groups to connect two Cu^{II} ions, leaving the third cyanide group free. The Fe^{III} ion has a slightly distorted octahedral coordination geometry formed by three nitrogen atoms from the tridentate ligand Tp and three cyanide carbon atoms. The Fe−C bond (1.912(5)−1.932(5) Å) and Fe−N bond (1.957(4)−1.985(4) Å) lengths in **1** are close to those in low-spin cyano-containing Fe^{III} complexes.[11−16,24] The Fe−C≡N bond angles are in the range of 174.5(4)−177.2(5)°, slightly deviated from 180°. The Cu^{II} ion has a distorted square pyramidal coordination geometry, where one $[TpFe(CN)_3]^-$ unit is bound to the basal site (Cu1−N9, 1.997(4) Å) and the other is bound to the elongated apical site (Cu1−N7a, 2.247(4) Å, symmetry code a: $2-x, -y, 1-z$). The remaining three basal sites are occupied by one oxygen atom from terephthalate and two nitrogen atoms from the ligand dmbpy with an average $Cu-N_{dmbpy}$ bond length of 2.013(9) Å and Cu1−O1 bond length of 1.930(3) Å. The C≡N−Cu bond angles, 159.5(3)° for C12≡N9−Cu1 and 150.6(4)° for C10≡N7−Cu1a, significantly deviate from linearity. The edge lengths of the rectangle (i.e., Fe···Cu distances) are 5.128 and 4.955 Å, and Fe···Fe and Cu···Cu distances are 7.219 and 7.043 Å, respectively. The size of the rectangle is of the same order as those of cyano-bridged Fe_2Cu_2 rectangular clusters reported before.[12b,c] The rectangular $[(Tp)_2Fe_2(CN)_6Cu_2(dmbpy)_2]^{2+}$ units are further connected via terephthalate dianion (ta) to form an interesting 1D chain. Each ta links two Cu^{II} ions of two neighboring rectangular units in an amphimonodentate coordination mode with Cu···Cu separation of 11.022 Å. The shortest interchain Cu···Cu, Fe···Cu, and Fe···Fe distances are 8.617, 9.110, and 11.868 Å, respectively.

The Oak Ridge thermal ellipsoid plot (ORTEP) view for complex **2** is shown in Figure 2. It is a pentanuclear cluster. In the cluster, each $[(Tp)Fe(CN)_3]^-$ unit provides one of three cyanide ligands to connect the Cu^{II} ion. The Fe^{III} ion is hexa-coordinated in the approximately octahedral geometry. The Fe−C and Fe−N bond lengths are in the range of 1.891(5)−2.047(4) Å and 1.887(3)−2.010(3) Å, respectively, which is comparable with the lengths reported in the low-spin Fe^{III} complexes.[11−16] The coordination spheres of Cu^{II} ions (for Cu1 and

(24) Gu, Z. G.; Liu, W.; Yang, Q. F.; Zhou, X.-H.; Zuo, J. L.; You, X. Z. *Inorg. Chem.* **2007**, *46*, 3236.

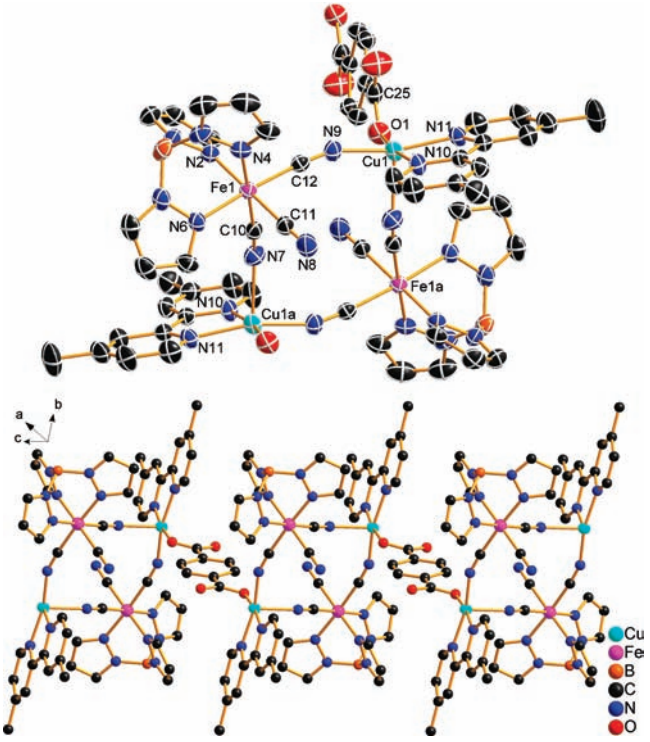

Figure 1. Structure segments of the 1D chain complex **1**. Thermal ellipsoids are drawn at the 50% probability level. The hydrogen atoms and solvated molecules are omitted for clarity (top). A perspective view of the 1D chain (bottom).

Cu2) can be described as a slightly distorted square pyramid. For Cu1, the environment is defined by two nitrogen atoms from the auxiliary ligand phen, one nitrogen atom from cyanide group, one oxygen atom from terephthalate in the basal plane, and one oxygen atom (O6) from one water molecule in the axial site. While for Cu2, the environment is composed of two nitrogen atoms from the auxiliary ligand phen, two oxygen atoms from two terephthalate ligands in the basal plane, and one oxygen atom (O5) from a methanol molecular in the axial site. The Cu1 ion is linked to Fe1 and Cu2 ions by cyanide and terephthalate, respectively, forming a V-shaped moiety. The symmetry-equivalent moiety is produced by a mirror plane through the Cu2 ion to lead to a W-shaped pentanuclear cluster. The Cu−N and Cu−O bond lengths are in the range of 1.990(3)−2.302(3) Å for Cu1, 1.986(3)−2.253(4) Å for Cu2, respectively. The C10≡N7−Cu1 bond angle (176.6(4)°) is nearly linear, which is comparable to the reported values[6e,12c] but much larger than those of **1**. The Cu1···Cu2 separation of 10.735 Å results from the long ta bridge. The shortest intramolecular Cu···Cu, Fe···Cu, and Fe···Fe distances are 10.735, 5.004, and 25.015 Å, respectively, while the shortest intermolecular Cu···Cu, Fe···Cu, and Fe···Fe distances are 12.200, 8.296, and 8.503 Å, respectively. The pentanuclear clusters strongly interact with each other through O−H···N, C−H···N, and C−H···O intermolecular hydrogen-bond interactions (Supporting Information, Table S1), leading to a 3D supramolecular framework (Figure 2).

Complex **3** is a tetranuclear Fe_2Cu_2 cluster (Figure 3). Each tailored tricyanometalate $[(i\text{-BuTp})Fe(CN)_3]^-$ is coordinated to Cu^{II} ion in monodentate mode to form a FeCu dimer, and two dimers are further connected via the ta bridge to lead to a Z-shaped tetranuclear cluster. The Fe^{III} ion lies in a slightly distorted octahedral coordination environment. The distances of Fe−C and Fe−N bonds are in the range of 1.906(4)−1.923(4) Å and 1.951(3)−1.965(3) Å, respectively, which are in good agreement with those in reported complexes containing the $[(i\text{-BuTp})Fe(CN)_3]^-$ precursor.[12b] The Fe−C≡N bond angles vary from 175.3(3) to 178.2(4)°, deviating from 180° slightly. The Cu^{II} ion is penta-coordinated as a slightly distorted square pyramid. The bottom plane of square pyramid is described by one oxygen atom of terephthalate, one nitrogen atom from the cyanide group of $[(i\text{-BuTp})Fe(CN)_3]^-$, and two nitrogen atoms of the auxiliary phen ligand. The axial position is occupied by one oxygen atom (O3) from an ethanol molecule with the Cu−O bond length of 2.218(3) Å. The bond lengths between Cu^{II} atom and atoms of the bottom plane of square−pyramid are among 1.901(3)−2.021(3) Å. The C≡N−Cu bond angle (172.6(3)°) is slightly deviated from linearity. The shortest intramolecular Cu···Cu, Fe···Cu, and Fe···Fe distances are 10.951, 4.977, and 15.356 Å, respectively, while the shortest intermolecular Cu···Cu, Fe···Cu, and Fe···Fe distances are 9.569, 7.468, and 9.569 Å, respectively.

For complexes **1**−**3**, the variation of structures from a 1D chain polymer to tetranuclear or pentanuclear clusters is ascribed to the difference of auxiliary ligands and tricyanometalate precursors. Among them, the steric effect may play an important role for the aggregations of the molecules.

The synthesis of microporous magnets at room temperature is still an open challenge for chemists, which is potentially useful in magnetic separations.[25] The synthetic approach presented in this paper, that is, using the mixed bridging ligands of rigid carboxylates and cyanometalates to connect paramagnetic ions, is perhaps useful for the assembly of series of new interesting porous magnets.

Magnetic Properties. The susceptibility variation at different temperatures of complex **1** was measured at 1.8−300 K under 2 kOe (Figure 4). At room temperature, the $\chi_M T$ value is 1.98 emu K mol^{-1}, which is higher than the spin-only value of 1.50 emu K mol^{-1} on the basis of two low-spin Fe^{III} ($S = 1/2$) and two Cu^{II} ($S = 1/2$) ions in the absence of any exchange coupling ($g_{Fe} = g_{Cu} = 2.0$). As the temperature decreases, $\chi_M T$ gradually increases and reaches a maximum of 2.41 emu K mol^{-1} at 8.5 K, suggesting that the cyanides mediate ferromagnetic coupling between Cu^{II} and Fe^{III} ions. Below 8.5 K, $\chi_M T$ sharply drops to 0.96 emu K mol^{-1} at 1.8 K, which may be attributed to the presence of significant zero-field splitting in the ground state, antiferromagnetic coupling between intrachain Fe_2Cu_2 rectangular units mediated by terephthalate groups, and/or interchain antiferromagnetic interactions. The Cu ions bridged by ta in amphimonodentate mode are well separated from each other (Cu···Cu ≈ 11 Å), which leads to weak antiferromagnetic interactions between metal centers,[26] and thus the Fe_2Cu_2

(25) (a) Milon, J.; Daniel, M. C.; Kaiba, A.; Guionneau, P.; Brandès, S.; Sutter, J. P. *J. Am. Chem. Soc.* **2007**, *129*, 13872. (b) Kaye, S. S.; Long, J. R. *J. Am. Chem. Soc.* **2005**, *127*, 6506.

(26) Deakin, L.; Arif, A. M.; Miller, J. S. *Inorg. Chem.* **1999**, *38*, 5072.

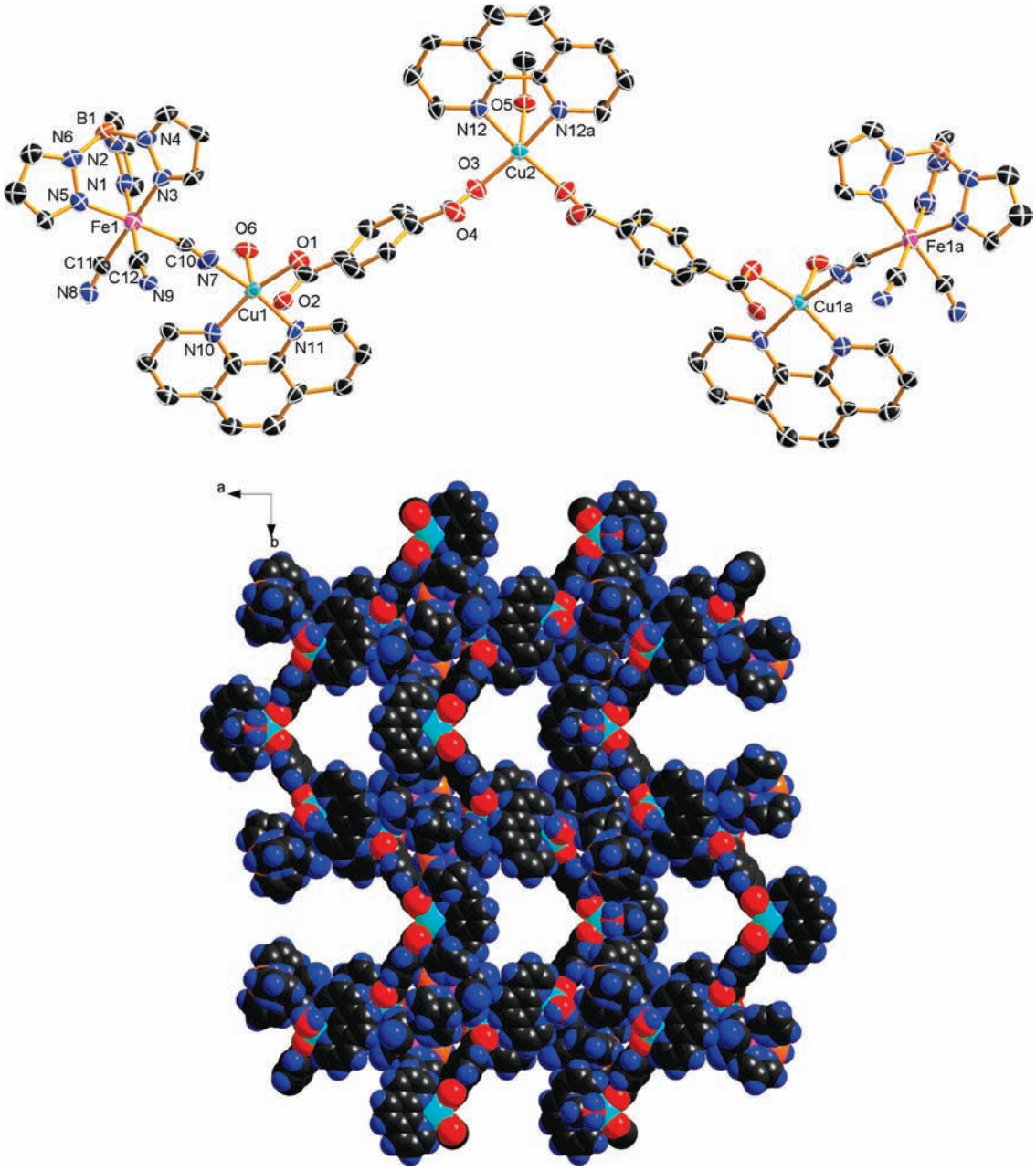

Figure 2. ORTEP view of the crystal structure for complex **2** showing the atom numbering scheme. Thermal ellipsoids are drawn at the 50% probability level. The hydrogen atoms and noncoordinated solvated molecules are omitted for clarity (top). The view of 3D supramolecular framework through intermolecular hydrogen-bond interactions excluding the solvated molecules (bottom).

rectangular units can be nearly considered to be magnetically isolated from each other. Therefore, a rectangular tetranuclear model that takes the intercluster interaction (zJ') in to account was used here: $\hat{H} = -2J[\hat{S}_{\mathrm{FeI}}(\hat{S}_{\mathrm{CuI}} + \hat{S}_{\mathrm{CuIA}}) + \hat{S}_{\mathrm{FeIA}}(\hat{S}_{\mathrm{CuI}} + \hat{S}_{\mathrm{CuIA}})]$, where J is the nearest-neighbor exchange constant mediated by cyanide in tetranuclear Fe_2Cu_2 cluster, and the Van Vleck expression is

$$\chi_{\mathrm{tetra}} = \frac{2Ng^2\beta^2}{kT} \times \frac{2 + e^{-2J/kT} + 5e^{2J/kT}}{7 + e^{-4J/kT} + 3e^{-2J/kT} + 5e^{2J/kT}} \quad (1)$$

$$\chi_{\mathrm{M}} = \frac{\chi_{\mathrm{tetra}}}{1 - (2zJ'/Ng^2\beta^2)\chi_{\mathrm{tetra}}} \quad (2)$$

The best fit between 8.5 and 300 K gives $g = 2.29$, $J = +2.08$ cm^{-1}, and $zJ' = -0.18$ cm^{-1} with $R = \sum[\chi_M T)_{\mathrm{calc}} - (\chi_M T)_{\mathrm{obs}}]^2/\sum(\chi_M T)^2_{\mathrm{obs}} = 1.3 \times 10^{-4}$. The large g factor can be ascribed to a combination of the orbital contributions from the low-spin Fe^{III} centers[10,15,27] and individual factors of >2 associated with the Cu^{II} centers, and is in good agreement with those reported previously in the similar systems.[6e,f,12a−c,28] The magnitude of the ferromagnetic coupling is somewhat lower than the values (11.91 and 8.90 cm^{-1}) estimated for the rectangular

(27) (a) Martin, L. L.; Martin, R. L.; Murray, K. S.; Sargeson, A. M. *Inorg. Chem.* **1990**, *29*, 1387. (b) Lescouëzec, R.; Lloret, F.; Julve, M.; Vaissermann, J.; Verdaguer, M.; Llusar, R.; Uriel, S. *Inorg. Chem.* **2001**, *40*, 2065.
(28) Wang, C. F.; Gu, Z. G.; Lu, X. M.; Zuo, J. L.; You, X. Z. *Inorg. Chem.* **2008**, *47*, 7957.

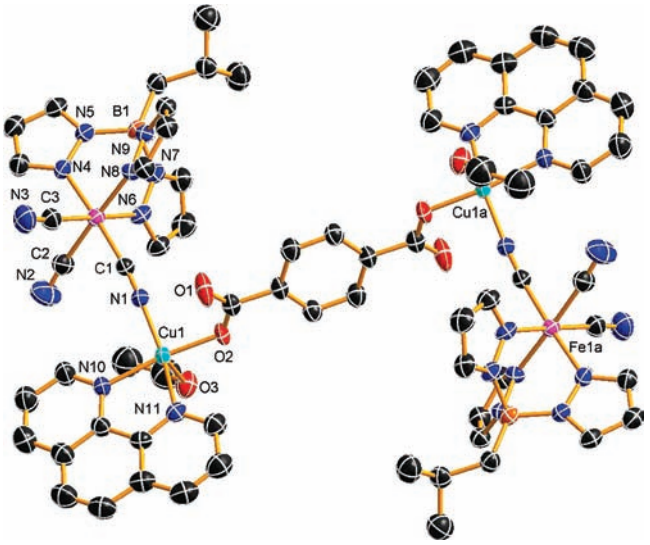

Figure 3. ORTEP view of the crystal structure for complex **3** showing the atom numbering scheme. Thermal ellipsoids are drawn at the 50% probability level. The hydrogen atoms and noncoordinated solvated molecules are omitted for clarity.

clusters $[(Tp)Fe(CN)_3Cu(Tp)]_2 \cdot 2H_2O$ and $[(PhTp)Fe(CN)_3Cu(bpy)(H_2O)(ClO_4)]_2 \cdot 2H_2O$ (PhTp = tris(pyrazolyl)phenylborate; bpy = 2,2′-bipyridine),[12b,c] but slightly larger than the value of 1.38 cm^{-1} observed for another rectangular cluster $[(Tp)Fe(CN)_3Cu(bpca)]_2 \cdot 4H_2O$ (bpca = bis(2-pyridylcarbonyl)amidate anion).[12c]

The magnetic susceptibility of **1** is field dependent at very low temperature (see inset of Figure 4). A maximum of χ_M was observed at 2.5 K under 1 kOe, indicating antiferromagnetism of **1** under this condition. The maximum broadens and shifts to lower temperature as the magnetic field increases, and it finally disappears for $H \geq 1.2$ T. This behavior shows the existence of a field induced transition from an antiferromagnetic ground state to a ferromagnetic state. Supporting Information, Figure S1 shows the variable-field magnetization of **1** at 1.8 K. The unsaturated magnetization value of 3.73 $N\mu_B$ at 7 T corresponds to the expected spontaneous magnetization of 4 $N\mu_B$ for the parallel ordering of unpaired electrons of the Fe_2Cu_2 unit, which confirms ferromagnetic coupling between the Cu^{II} and Fe^{III} centers. The sigmoid shape of the magnetization (M) versus field (H) plot further confirms the meta-magnetic behavior of **1**. From the variable-field (Supporting Information, Figure S1) and variable-temperature magnetization measurements at low fields (inset of Figure 4), the critical field is estimated to be about 1.2 T. According to the crystal structure of complex **1**, this metamagnetic behavior can be attributed to the coexistence of intracluster Fe_2Cu_2 ferromagnetic coupling and intercluster/interchain antiferromagnetic interactions. Similar magnetic behavior has been reported previously in the neutral cyano-bridged chain complex, $\{[Fe^{III}{}_2(bpym)_2(CN)_8Cu^{II}(H_2O)_2] \cdot 6H_2O\}_n$.[29] When $H_{dc} = 0$, a peak was observed at 2.5 K in the in-phase variable-temperature magnetization, m', but the out-of-phase variable-temperature magnetization, m'', is

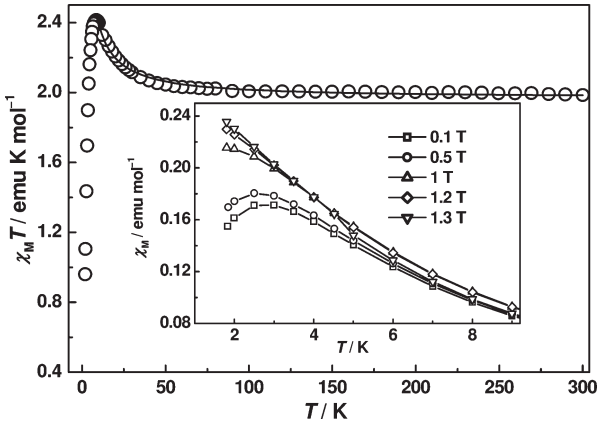

Figure 4. Temperature dependence of $\chi_M T$ for complex **1** at 2 kOe (the solid line represents the fitting to the data). Inset: Field dependence of the magnetic susceptibility of **1** at low temperatures under the applied field varying in the range 1 kOe to 1.3 T (the solid lines are simply to guide the eye).

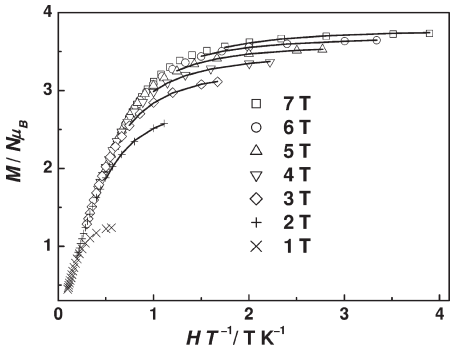

Figure 5. Plot of reduced magnetization, $M/N\mu_B$ (N is Avogadro's number and μ_B is the Bohr magneton) versus H/T for complex **1**. The solid lines represent the fitting to the data.

zero, suggesting antiferromagnetic ordering at this temperature (T_N, Supporting Information, Figure S2).

The magnetization data at a variety of fields were recorded in the temperature range 1.8−10 K (Figure 5). The non-superposition of the isofield lines indicates the presence of significant zero-field splitting. With the spin ground state $S = 2$, fits of the data using ANISOFIT[30] afford zero-field splitting parameter of $D = -1.48$ cm^{-1} with $g = 1.96$. The small Landé splitting may be attributed to the non-negligible population of low-lying excited states and/or antiferromagnetic interaction.

The temperature dependence of susceptibility for complex **2** is shown in Figure 6. At room temperature, the $\chi_M T$ value of 2.70 emu K mol^{-1} is higher than the value of 1.875 emu K mol^{-1} expected for a spin-only contribution from two low-spin Fe^{III} ($S = {}^1/_2$) and three Cu^{II} ($S = 1/2$) ions in the absence of any exchange coupling ($g_{Fe} = g_{Cu} = 2.0$), which can also be ascribed to a combination of the orbital contributions from the low-spin Fe^{III} centers and individual Landé factors of >2 associated with the Cu^{II} centers. As lowering the temperature, $\chi_M T$ rises to a maximum of 3.19 emu K mol^{-1} at about 8 K, after which point it decreases to 2.69 emu K mol^{-1} at 1.8 K. This magnetic behavior is indicative of the expected ferromagnetic

(29) Toma, L. M.; Lescouëzec, R.; Pasán, J.; Ruiz-Pérez, C.; Vaissermann, J.; Cano, J.; Carrasco, R.; Wernsdorfer, W.; Lloret, F.; Julve, M. *J. Am. Chem. Soc.* **2006**, *128*, 4842.

(30) Shores, M. P.; Sokol, J. J.; Long, J. R. *J. Am. Chem. Soc.* **2002**, *124*, 2279.

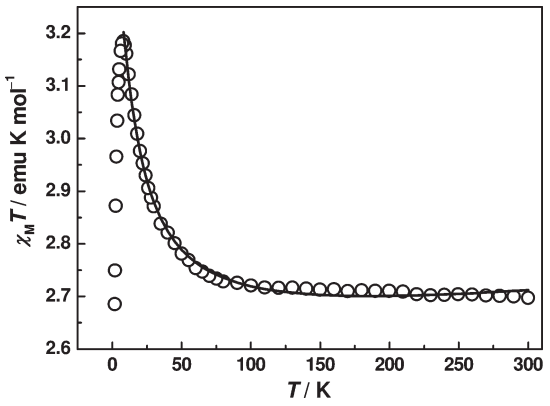

Figure 6. Temperature dependence of $\chi_M T$ for complex **2** at 2 kOe. The solid line represents the fitting to the data.

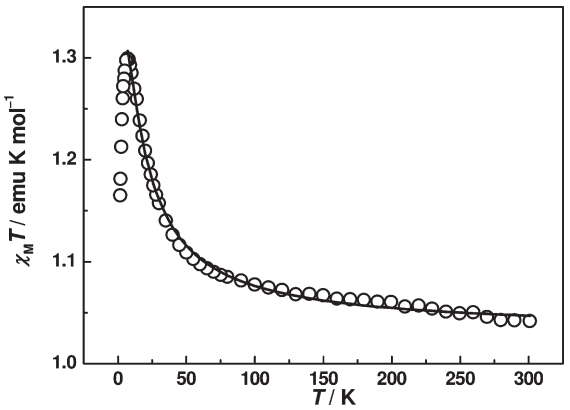

Figure 7. Temperature dependence of $\chi_M T$ for complex **3** at 2 kOe. The solid line represents the fitting to the data.

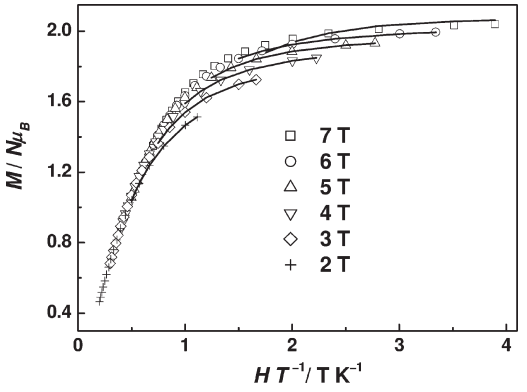

Figure 8. Plot of reduced magnetization, $M/N\mu_B$ (N is Avogadro's number and μ_B is the Bohr magneton) versus H/T for complex **3**. The solid lines represent the fitting to the data.

interactions between the Fe^{III} and the Cu^{II} ions, which is further confirmed by the unsaturated magnetization value of 5.19 $N\mu_B$ under the 7 T magnetic field at 1.8 K (Supporting Information, Figure S3). According to the structure, a magnetic model involving two FeCu dimers and one paramagnetic Cu center was used here, and the susceptibilities expression can be written as follows:

$$\chi_m = 2\chi_{FeCu} + \chi_{Cu} = \frac{4Ng^2\beta^2}{kT} \times \frac{1}{3 + e^{-2J/kT}} + \frac{Ng^2\beta^2}{4kT} + \text{TIP} \qquad (3)$$

A molecular field approximation was taken into account for the intermolecular interaction (zJ') as eq 2. Fitting the $\chi_M T$ data above 8 K gave $g = 2.36$, $J = +6.45$ cm^{-1}, TIP $= 2.6 \times 10^{-4}$ emu mol^{-1}, $zJ' = -0.0039$ cm^{-1} with $R = 7 \times 10^{-5}$.

The temperature variation of susceptibility for complex **3** is displayed in Figure 7, χ_M being the magnetic susceptibility per FeCu unit. As the temperature is lowered, the $\chi_M T$ value increases gradually from room temperature value of 1.06 emu K mol^{-1}, and then reaches a maximum of 1.30 emu K mol^{-1} at 7 K, suggesting the ferromagnetic interactions between the Fe^{III} and Cu^{II} ions. This magnetic behavior is confirmed by the field-dependent magnetization, which exhibit the nearly saturated magnetization values of 2.04 $N\mu_B$ at 7 T (Supporting Information, Figure S4). Under 7 K, $\chi_M T$ decreases, indicating the presence of zero-field splitting and/or weak intermolecular antiferromagnetic interactions. Fitting the $\chi_M T$ data using the isotropic spin Hamiltonian $\hat{H} = -2J\hat{S}_{Fe}\hat{S}_{Cu}$, including the intermolecular interactions (zJ'), gave $g = 2.34$, $J = +6.54$ cm^{-1} and $zJ' = -0.11$ cm^{-1} with $R = 2.0 \times 10^{-5}$. The magnitude of the ferromagnetic coupling for **3** is comparable to that for **2**. The field dependence of the magnetization for **3** at temperature between 1.8 and 10 K is shown as the M versus H/T plots in Figure 8. The non-superposition of the isofield lines confirms the presence of significant zero-field splitting. With the spin ground state $S = 1$, fits of the magnetization data using ANISOFIT[30] afford a zero-field splitting parameter of $D = -6.34$ cm^{-1} with $g = 2.40$.

Conclusions. Using the tricyanometalate and terephthalate units as the mixed bridging ligands, three interesting heterometallic complexes, including the 1D chain polymer $\{[(Tp)_2Fe_2(CN)_6Cu_2(ta)(dmbpy)_2]\cdot 7H_2O\}_n$ (**1**), the pentanuclear heterometallic cluster $[(Tp)_2Fe_2(CN)_6Cu_3(phen)_3(ta)_2(MeOH)(H_2O)_2]\cdot 8H_2O$ (**2**), and the tetranuclear heterometallic cluster $[(i\text{-BuTp})_2Fe_2(CN)_6Cu_2(ta)(phen)_2(EtOH)_2]\cdot 2MeOH\cdot H_2O$ (**3**), have been successfully synthesized and structurally characterized. The structural differences of these complexes result from the different auxiliary ligands and tricyanometalate building blocks. Complex **2** shows a 3D supramolecular framework through intermolecular hydrogen-bond interactions. All complexes show ferromagnetic interactions between the Fe^{III} and Cu^{II} ions. Complex **1** shows metamagnetic behavior with the critical field of 1.2 T at 1.8 K. The synthetic approach of using the mixed bridging ligands of rigid carboxylates and cyanometalates to connect paramagnetic ions can be useful for the further chemical studies on new porous magnets.

Acknowledgment. This work was supported by the National Science Fund for Distinguished Young Scholars (20725104), the Major State Basic Research Development Program (2006CB806104 and 2007CB925100), and the National Natural Science Foundation of China (20721002).

Supporting Information Available: Additional structure and magnetic characterization data (PDF), and X-ray crystallographic files in CIF format for **1**−**3**. This material is available free of charge via the Internet at http://pubs.acs.org.